RSC Advances

PAPER

View Article Online
View Journal | View Issue

Cite this: *RSC Adv.*, 2024, **14**, 18103

An ethyl cellulose novel biodegradable flexible substrate material for sustainable screen-printing

Elena Palmieri,†[a] Rocco Cancelliere, †*[b] Francesco Maita,*[a] Laura Micheli [b] and Luca Maiolo[a]

We introduce an innovative solution to reduce plastic dependence in flexible electronics: a biodegradable, water-resistant, and flexible cellulose-based substrate for crafting electrochemical printed platforms. This sustainable material based on ethyl cellulose (EC) serves as an eco-friendly alternative to PET in screen printing, boasting superior water resistance compared to other biodegradable options. Our study evaluates the performance of carbon-based screen-printed electrodes (SPEs) fabricated on conventional PET, recycled PET (r-PET), and (EC)-based materials. Electrochemical characterization reveals that EC-SPEs exhibit comparable analytical performance to both P-SPEs and rP-SPEs, as evidenced by similar limits of detection (LOD), limits of quantification (LOQ), and reproducibility values for all the analytes tested (ferro-ferricyanide, hexaammineruthenium chloride, uric acid, and hydroquinone). This finding underscores the potential of our cellulose-based substrate to match the performance of conventional PET-based electrodes. Moreover, the scalability and low-energy requirements of our fabrication process highlight the potential of this material to revolutionize eco-conscious manufacturing. By offering a sustainable alternative without compromising performance, our cellulose-based substrate paves the way for greener practices in flexible electronics production.

Received 22nd April 2024
Accepted 30th May 2024

DOI: 10.1039/d4ra02993c

rsc.li/rsc-advances

Introduction

Screen printing has emerged as a prominent method for producing flexible electronics, owing to its versatility across various substrates, cost-effectiveness, and scalability for large-scale manufacturing. Notably, it facilitates rapid prototyping and customisation, although it faces challenges such as lower resolution compared to photolithography, and variations in layer thickness affecting device performance.[1–5] Despite these limitations, screen printing remains significant in flexible electronics, balancing accessibility, and feasibility, especially in applications like wearable technology and sensors.

Several polymeric substrates are used in flexible electronics due to their compatibility with screen printing. Examples[6–12] include polyethene terephthalate (PET), polyethene naphthalate (PEN), and polyimide (PI). The quest for alternative materials in screen printing aims to replace these conventional substrates since they come from non-renewable sources. Biodegradable polymers like polylactic acid (PLA)[13,14] and cellulose-based materials offer eco-friendly alternatives[15–17] to used-to-date polymeric substrates. PLA, sourced from renewable materials such as maise starch, demonstrates excellent printability and biodegradability. Meanwhile, paper-based screen-printed electrodes have seen extensive application in recent decades. Indeed, paper-based electrodes have demonstrated performance comparable to that of PET electrodes in sensing diverse analytes.[18] Nevertheless, challenges persist in their utilisation. For instance, paper requires a wax coating to facilitate the printing process[19] and to delimit the electrode and the reaction zones, potentially impacting electrode recyclability. Occasionally, the employment of non-environmentally friendly chemicals or procedures becomes necessary to enhance the processability of the substrate.[20] Moreover, its sensitivity to water poses limitations on certain applications[21,22] and raises concerns regarding electrode storage in uncontrolled environments. Despite these hurdles, the versatility and sustainability of paper-based electrodes offer promising avenues for future development in flexible[23] electronics, although PET is still the most commonly used substrate. In this regard, to address the growing environmental concerns associated with disposable plastic-based devices, a recent proposal has been to utilise recycled PET for manufacturing screen-printed electrodes (SPEs). This initiative aligns with the objectives outlined in the European Union's "European Strategy for Plastics in a Circular Economy," which aims to ensure that by 2030, all plastic packaging introduced to the EU market will be either easily reusable or recyclable at minimal cost.[24]

[a]*Istituto per la Microelettronica e i Microsistemi, Consiglio Nazionale delle Ricerche, Via del Fosso del Cavaliere 100, Rome 00133, Italy. E-mail: francesco.maita@cnr.it*

[b]*Department of Chemical Science and Technologies, University of Rome Tor Vergata, Via della Ricerca Scientifica 1, Rome 00133, Italy. E-mail: rocco.cancelliere@uniroma2.it*

† These authors equally contributed to the paper.

In this quest for greener solutions, we introduce ethyl cellulose (EC),[25,26] a bio-friendly option, as a game-changer for creating transparent, flexible and water-resistant substrates for electrochemical printed platforms. This material is suitable for eco-conscious manufacturing methods like roll-to-roll processes and printing. Plus, it can be exploited for the fabrication of devices using advanced techniques like photolithography,[25,26] paving the way for its industrial use. Moreover, the one-step room temperature process makes EC a good candidate as a flexible electronic substrate material since it reduces further the energy needed to fabricate bendable devices, and the substrates can withstand up to 2500 bending cycles.[26] The reduction of the environmental impact associated with traditional substrates would contribute to a more sustainable approach to the use of disposable devices. Therefore, we exploited this novel material for the fabrication of screen-printed electrodes, and we compared the performances of SPEs fabricated on EC (EC-SPE), commercial PET (P-SPE), and recycled PET (rP-SPE).

Experimental

Materials and methods

Ethyl cellulose (EC) with 48–49.5% ethoxy content was purchased from Sigma. All the solvents used were purchased from Sigma. Sodium nitrite, hydroquinone, L-ascorbic acid, uric acid, and potassium chloride were supplied by Sigma-Aldrich (Steinheim, Germany). Ferrocyanide and potassium ferricyanide were supplied from Fluka Chemie, Sigma-Aldrich (Buchs, Switzerland). The buffer solutions were 0.05 M phosphate-buffered saline (PBS) + 0.1 M KCl with a pH of 7.4 and 0.05 M carbonate buffer (CB) with a pH of 9.0.

EC dispersion was prepared by dissolving it in ethanol and stirring at 45 °C until dissolution. The EC substrate is prepared at room temperature *via* solvent casting method from a 10% w ethanol-based dispersion. The full procedure and characterisation of the film are reported in a previous work[24] and summarised in Fig. 1.

The in-house production of SPEs was conducted using a 245 DEK high-performance, multi-purpose, precision screen-printing machine. The working electrode (WE) with a geometric area of approximately 0.07 cm^2 and the counter electrodes (CEs) were printed using graphite-based ink (Elettrodag 421 cured at 80 °C), while the reference electrode (RE) was printed using silver ink (cured at 80 °C).

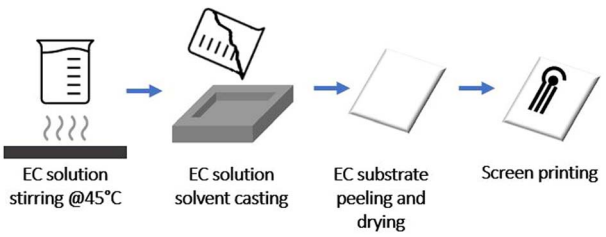

Fig. 1 Outline of the main steps of the fabrication of the EC-SPEs.

UV-vis spectroscopy was conducted utilizing a PerkinElmer Lambda 35 UV/vis spectrometer, capturing spectra ranging from 1100 to 200 nm with a resolution of 4 nm.

FTIR-ATR characterization was carried out using a Thermo-Scientific Nicolet Summit spectrometer in absorbance mode. Samples were analyzed in attenuated total reflectance mode (ATR), utilizing a diamond crystal as a reflection accessory. The spectra were recorded from 3700 to 500 cm^{-1} with a resolution of 2 cm^{-1}.

Optical images and profilometry characterization were conducted in collaboration with SIMITECNO SRL using the Interferometer TopMap Micro.View+ Polytec.

Results and discussion

Characterisation of the material

The chemical stability of the novel EC-based material and its mechanical performances were extensively examined in a prior study,[26] and we gained insights into its limitations and advantages compared to other biomaterials and conventional petroleum-based materials. The clear benefit of EC over typical PET substrates lies in its biodegradability. What sets EC apart from other biodegradable cellulose-based options like paper is its exceptional water resistance, allowing for prolonged analyte measurements in aqueous environments without compromising electrode functionality, even when stored or subjected to uncontrolled environmental conditions. Remarkably, the material retains its integrity when immersed in water or exposed to sunlight, even after a few years, despite being biodegradable. To validate that the EC films we obtained exhibit properties consistent with those reported in the literature,[27,28] EC samples were submerged in distilled water and placed on a windowsill, subjecting them to natural environmental conditions, in order to simulate and highlight uncontrolled storage conditions. Periodically, the EC samples were taken out of the water, dried with compressed air, and then monitored for weight changes. Additionally, they underwent FTIR-ATR and UV-vis characterization to assess any potential degradation. Regarding weight monitoring, no fluctuations in weight were observed, while FTIR-ATR and UV-vis spectra of the substrate before and after being immersed in water for one year are reported respectively in Fig. 2a and b. The FTIR-ATR spectra reported in Fig. 2a revealed the features reassumed in Table 1.[29,30]

Notably, there were no significant differences observed between the spectra before and after treatment with water. No signs of cellulose degradation or oxidation were detected. Furthermore, there was no alteration observed in the band at 1650 cm^{-1}, indicative of –OH bending from absorbed water molecules, in the water-treated sample, and no variation occurred to the band at around 3500 cm^{-1} of the hydroxyl groups. UV-vis transmission analysis showed that no significant variation in the transmittance of the EC substrate was observed after water treatment (Fig. 2b). Otherwise, if the cellulose is susceptible to water, swelling phenomena and changes in transparency and colour could happen.[31] Despite its stability in water, it is biodegradable. Its biodegradability was monitored *via* periodical weight measurements of EC samples placed in

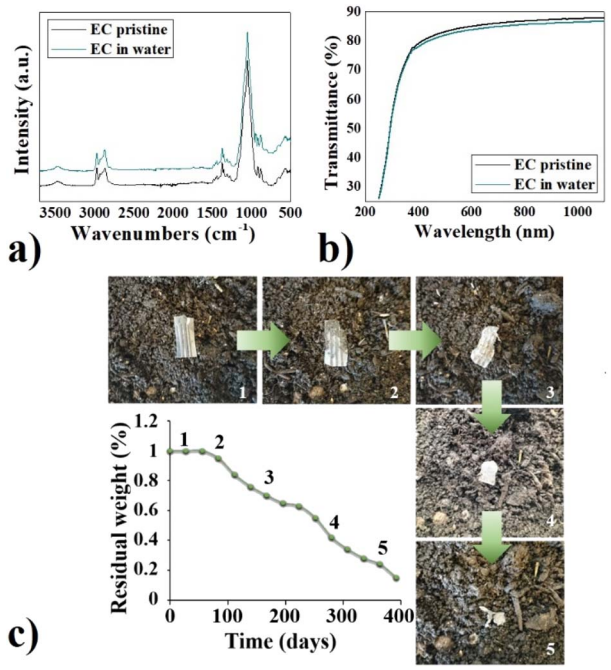

Fig. 2 EC water stability: (a) FTIR-ATR spectra and (b) UV-vis spectra of pristine EC and after one year in water. (c) EC-SPE biodegradability: pictures of SPEs on EC at various degradation states and a graph showing the biodegradability rate.

Table 1 FTIR spectra features

Wavenumber (cm^{-1})	Attribution
1050	C–O–C vibration of pyranose ring
2900 and 137	–CH stretching and deformation vibrations
1200–1500	–CH bending
500–800	–OH out-of-plane bending
1650	–OH bending of absorbed water molecules
3400	–OH groups stretching

common soil and compost. It required more than a year to degrade in soil (Fig. 2c), while shorter time if properly composted (3 to 10 months, depending on the compositing conditions).

From this perspective, this cellulose-based material exhibits comparable behaviour to PLA, one of the most prevalent bioplastics utilized in various industries such as biomedical, textile, and packaging.[32,33]

The morphology of the substrates used for the fabrication of the SPEs, *i.e.* PET, r-PET and EC, underwent characterisation through electronic and optical microscopy. Optical images and profilometry characterization are reported in Fig. 3. While the morphologies of the three substrates exhibit similarities, some distinctions are noticeable. The electrode border is notably sharper for the PET substrate. Conversely, both EC and r-PET display borders with minor defects and less distinct margins, probably due to the different substrate wettability.

Additionally, r-PET exhibits evident signs of surface irregularities due to its recycled packaging nature, whereas the morphologies of the other two substrates remain uniform. Furthermore, the roughness of the different materials was examined through profilometry analysis. The Sq (root mean square height) values, obtained from mapping a 0.2 cm^2 area of each substrate, are 0.26 μm for r-PET, 0.13 μm for PET, and 0.1 μm for EC, while the Sa (arithmetical mean height) values are 0.17 μm for r-PET, 0.09 μm for PET, and 0.07 μm for EC. This demonstrates that our cellulose-based substrate possesses a roughness level comparable to commercial PET.

Electrochemical characterisation of the electrodes

An extensive electrochemical characterisation was performed to verify the performance of the developed electrodes. To that end, the background current of P-SPEs, rP-SPE and EC-SPE was measured through chronoamperometry (0.4 V the oxidation peak of the Fe^{2+}, 180 s) in 50 mM KCl solution. The recorded currents were 30 ± 4 nA for P-SPEs, 35 ± 5 nA for rP-SPEs, and 36 ± 4 nA for EC-SPEs ($n = 6$ electrodes for each electrode type), respectively.

After that, the signal-to-noise ratios (S/N) corresponding to the current measured in the presence (10 mM $Fe(CN)_6^{3-/4-}$) and the absence (50 mM KCl, the one previously measured) of a redox probe were evaluated. S/N of 228 ± 19, 225 ± 20, and 230 ± 20 was obtained for P-SPEs, rP-SPEs, and EC-SPEs, respectively. With these first outcomes acquired, it is feasible to highlight significant comparability for all the platforms investigated. The electron transport and diffusivity processes at the electrode interface of EC-SPEs were studied using Electrochemical Impedance spectroscopy (EIS) and Cyclic Voltammetry (CV) with a 10 mM solution of $Fe(CN)_6^{3-/4-}$ as an electroactive probe. Fig. 4a and b display the relative CVs and Nyquist plot.

Initial visual inspection revealed that both the voltammetry and impedimetric analysis produced comparable results in terms of peak current (I_p), peak-to-peak separation (ΔE) and charge transfer resistance (R_{ct}). The numerical values of each electroanalytical parameter are provided in Table 2.

Initially, the diffusional process at the electrode/electrolyte interface was investigated. As previously detailed in our prior research, the diffusion coefficient (D_0) may be estimated by utilising the Randless Sevcik equation and the current peak (I_p) measured at a constant concentration of a redox probe (10 mM $Fe(CN)_6^{3-/4-}$).[34] D_0 is the mean value of the diffusion coefficient for the oxidation process (D_{ox}) of Fe^{2+} and the redox process of Fe^{3+} (D_{red}), determined from the cathodic current peak (I_{pc}). The D_0 values shown in Table 2 indicate that P-SPE, rP-SPE, and EC-SPE exhibited comparable diffusional behaviours. Moreover, comparing these results with the D_0 value reported in the literature by Konopka and McDuffy reveals a similar planar diffusion-controlled mechanism (about 10^{-6} magnitude) in the oxidation/reduction processes of $Fe(CN)_6^{3-/4-}$.[24] This behaviour is supported by the impedimetric results indicated by the W values obtained, which are the same for P-SPEs, rP-SPEs, and EC-SPEs. Afterwards, the electron transfer process was studied by comparing the current peak ratio (I_{pa}/I_{pc}), ΔE, and R_{ct}. For a reversible couple such as $Fe(CN)_6^{3-/4}$, the I_{pa}/I_{pc} is equal to one. The I_{pa}/I_{pc} ratios in Table 2 exhibit a strictly comparable behaviour for all the platforms evaluated. This is confirmed by

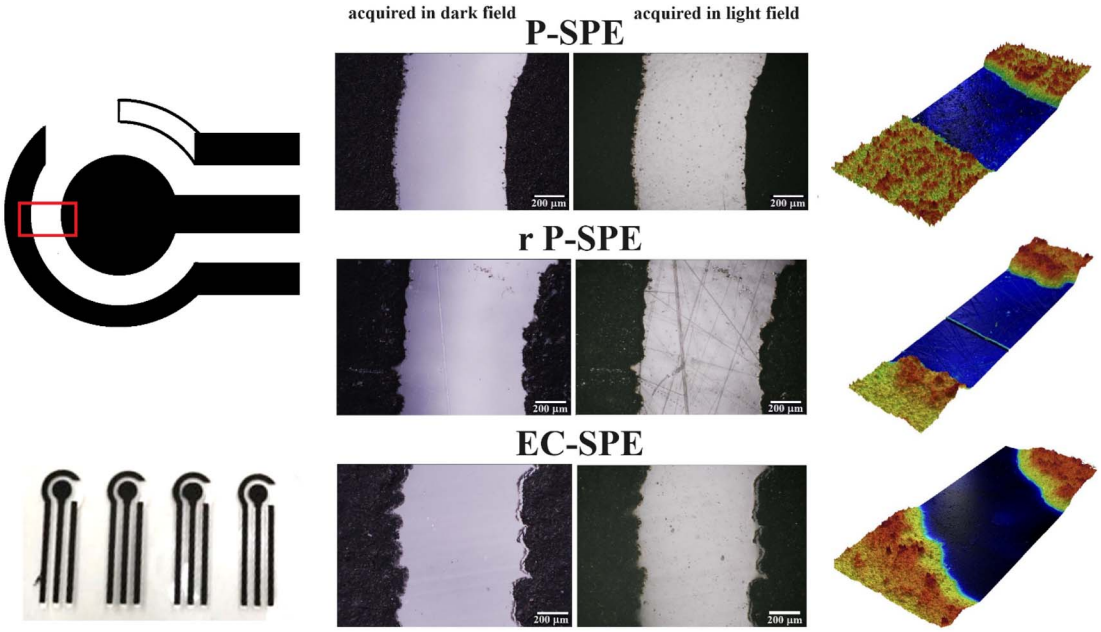

Fig. 3 Optical images, picture and 3D mapping of SPE printed on commercial PET (P-SPE), recycled PET (rP-SPE) and EC (EC-SPE).

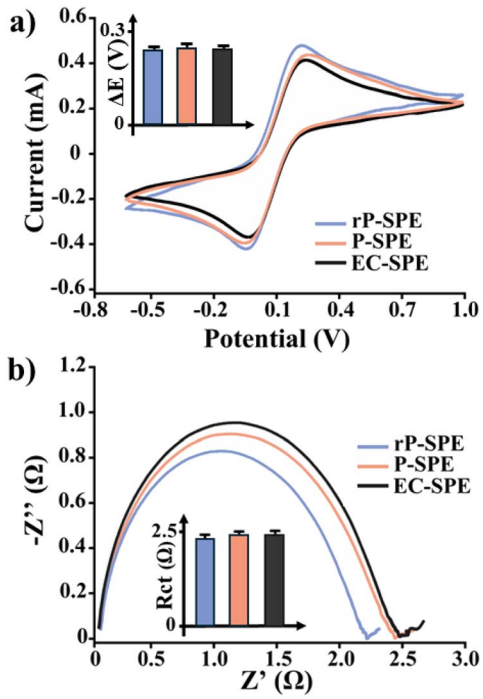

Fig. 4 Electrochemical characterisation of EC-SPE. In (a) and (b) similar conductivity of EC-SPEs compared to rP-SPE and P-SPE was determined using voltammetric and impedimetric characterization. Comparable ΔE and R_{ct} were obtained. The error bars reported are the standard deviation calculated on six independent electrodes for each tested platform.

ΔE values, which are always higher than 59 mV, thus suggesting a sluggish electron exchange.[35] This criterion is crucial for recognising Nernstian behaviour and calculating the number of electrons transferred. All platforms in this instance can be classified as a "quasi-reversible" system.[36] This phenomenon is characteristic of graphite-based screen-printed platforms. Many studies in the past decade have suggested modifying these platforms with nanomaterials. Our group achieved important results in this regard, by proposing multiwall nanotubes (MWNTs), graphene and biochar-modified SPEs for (bio) sensing purposes.[8,37]

Table 2 Comparison of the electrochemical parameters of P-SPE, rP-SPE and EC-SPE

$Fe(CN)_6^{3-/4-}$	P-SPE	rP-SPE	EC-SPE
I_{pa}/I_{pc}	0.9 ± 0.1	1.2 ± 0.1	1.2 ± 0.1
ΔE (V)	0.24 ± 0.02	0.27 ± 0.02	0.26 ± 0.02
$D_0 \times 10^{-6}$ ($cm^2\ s^{-1}$)	1.9 ± 0.3	1.5 ± 0.3	1.6 ± 0.3
R_{ct} (Ω)	2.2 ± 0.2	2.4 ± 0.2	2.4 ± 0.2
W (Kσ)	0.5 ± 0.1	0.5 ± 0.1	0.5 ± 0.1

After that, an in-depth investigation of the analytical performances of EC-SPE was conducted. Parameters such as limit of detection (LOD), limit of quantification (LOQ), sensitivity and reproducibility (RSD%) were evaluated by analysing electrochemical reversible and non-reversible redox probes. Ferro-ferricyanide, hexaammineruthenium chloride $Ru(NH_3)_6$-Cl, uric acid (UA), and hydroquinone (HQ) were utilised as probes, with square wave voltammetry (SWV) employed as the analytical method. The comparative outcomes are presented in Table 3.

These results demonstrate that EC-SPEs have identical analytical performance to P-SPEs and rP-SPEs, as evidenced by the comparable LOD, LOQ, and reproducibility values observed. Reproducibility was assessed by analysing six distinct

Table 3 Comparison of the analytical performances of P-SPE, rP-SPE and EC-SPE

	P-SPE	rP-SPE	EC-SPE
$Fe(CN)_6^{3-/4-}$			
LOD (μM)	9.4	10.7	10.3
LOQ (μM)	28.4	35.2	34.3
Sensitivity (mA/M cm^2)	40	42.4	41.3
Reproducibility (RSD%)	9	10	10
$Ru(NH_3)_6Cl$			
LOD (μM)	15.5	13.6	16.3
LOQ (μM)	51.4	47.4	53.8
Sensitivity (mA/M cm^2)	61.7	53.3	66.4
Reproducibility (RSD%)	10	10	11
UA			
LOD (μM)	7.1	6.8	7.0
LOQ (μM)	22.6	21.2	21.7
Sensitivity (mA/M cm^2)	44.3	37.4	42.1
Reproducibility (RSD%)	9	10	9
HQ			
LOD (μM)	8.8	9.5	10.1
LOQ (μM)	27.4	29.6	33.4
Sensitivity (mA/M cm^2)	40.6	41.8	46.3
Reproducibility (RSD%)	10	10	10

electrodes from each substrate, with similar relative standard deviations (RSD%): 10% for P-SPEs, 11% for rP-SPEs, and 10% for EC-SPEs.

Conclusions

Based on the data presented, it can be inferred that the newly developed biodegradable material utilizing ethyl cellulose (EC) is well-suited as a substrate for fabricating screen-printed electrodes (SPEs). The observed sensing performance is on par with that of SPEs printed on PET and recycled PET substrates. Additionally, the production process for EC-based substrates occurs at low temperatures and allows for standardization and scalability to produce, for instance, A4-sized sheets. These sheets could be a viable alternative to the commercially used sheets for fabricating PET electrodes. This flexible, transparent material maintains stability over a year but can biodegrade when composted correctly. This finding offers hope for substantially reducing the environmental impact of disposable devices, extending beyond screen-printed electrodes to encompass all devices produced through screen printing on flexible PET-like substrates. We reached results comparable to those on PET in terms of LOD, LOQ, sensitivity and reproducibility for all the analytes tested (ferro-ferricyanide, hexaammineruthenium chloride, uric acid, and hydroquinone). By guaranteeing consistent performance, it sets the stage for the development of greener and more effective electronic devices. This innovation addresses the pressing need for environmentally friendly materials and demonstrates the feasibility of transitioning towards more sustainable manufacturing processes.

Author contributions

Conceptualization – R. Cancelliere, E. Palmieri; data curation – R. Cancelliere, E. Palmieri; investigation – R. Cancelliere, E. Palmieri; methodology- E. Palmieri, R. Cancelliere; supervision – R. Cancelliere, L. Maiolo, F. Maita, L. Micheli; validation – L. Maiolo, F. Maita, L. Micheli; writing – original draft – E. Palmieri, R. Cancelliere; writing – review & editing – E. Palmieri, R. Cancelliere, L. Maiolo, F. Maita, L. Micheli.

Conflicts of interest

There are no conflicts to declare.

Notes and references

1 L. Maiolo, A. Pecora, F. Maita, A. Minotti, E. Zampetti, S. Pantalei, A. Macagnano, A. Bearzotti, D. Ricci and G. Fortunato, *Sens. Actuators, B*, 2012, **179**, 114.
2 D.-H. Kim, *Nature*, 2008, **320**, 507.
3 T. Someya, Z. Bao and G. G. Malliaras, *Nature*, 2016, **540**, 379.
4 P. Sodkrathok, C. Karuwan, W. Kamsong, A. Tuantranont and M. Amatatongchai, *Talanta*, 2023, **262**, 124695.
5 S. Nur Ashakirin, M. H. M. Zaid, M. A. S. M. Haniff, A. Masood and M. F. Mohd Razip Wee, *Measurement*, 2023, **210**, 112502.
6 M. Li, D. W. Li, G. Xiu and Y. T. Long, *Curr. Opin. Electrochem.*, 2017, **3**, 137.
7 A. Muhammad, R. Hajian, N. A. Yusof, N. Shams, J. Abdullah, P. M. Woi and H. Garmestani, *RSC Adv.*, 2018, **8**, 2714.
8 R. Cancelliere, A. Di Tinno, A. Cataldo, S. Bellucci and L. Micheli, *Biosensors*, 2022, **12**, 2.
9 Q. Li, J. Zhang, Q. Li, G. Li, X. Tian, Z. Luo, F. Qiao, X. Wu and J. Zhang, *Front. Mater.*, 2019, **5**, 1.
10 X. Gong, K. Huang, Y. H. Wu and X. S. Zhang, *Sens. Actuators, A*, 2022, **345**, 113821.
11 T. Pandhi, C. Cornwell, K. Fujimoto, P. Barnes, J. Cox, H. Xiong, P. H. Davis, H. Subbaraman, J. E. Koehne and D. Estrada, *RSC Adv.*, 2020, **10**, 38205.
12 S. Park, S. Ban, N. Zavanelli, A. E. Bunn, S. Kwon, H. R. Lim, W. H. Yeo and J. H. Kim, *ACS Appl. Mater. Interfaces*, 2023, **15**(1), 2092–2103.
13 P. S. Sfragano, S. Laschi and I. Palchetti, *Front. Chem.*, 2020, **8**, 1.
14 R. M. Cardoso, D. P. Rocha, R. G. Rocha, J. S. Stefano, R. A. B. Silva, E. M. Richter and R. A. A. Muñoz, *Anal. Chim. Acta*, 2020, **1132**, 10.
15 E. Jansson, J. Lyytikäinen, P. Tanninen, K. Eiroma, V. Leminen, K. Immonen and L. Hakola, *Materials*, 2022, **15**, 957.
16 C. M. Silveira, T. Monteiro and M. G. Almeida, *Biosensors*, 2016, **6**, 1.
17 S. Agate, M. Joyce, L. Lucia and L. Pal, *Carbohydr. Polym.*, 2018, **198**, 249.
18 N. Ruecha, R. Rangkupan, N. Rodthongkum and O. Chailapakul, *Biosens. Bioelectron.*, 2014, **52**, 13.

19 S. Cinti, M. Basso, D. Moscone and F. Arduini, *Anal. Chim. Acta*, 2017, **960**, 123.
20 S. Kang, Z. Li, J. Li, H. Wei, Y. Guo, H. Li, P. Yan and H. Wu, *Polymers*, 2023, **15**, 1.
21 A. Hauke, P. Simmers, Y. R. Ojha, B. D. Cameron, R. Ballweg, T. Zhang, N. Twine, M. Brothers, E. Gomez and J. Heikenfeld, *Lab Chip*, 2018, **18**, 3750.
22 E. C. Rama and M. T. F. Abedul, *Biosensors*, 2021, **11**, 1.
23 H. Eynaki, M. A. Kiani and H. Golmohammadi, *Nanoscale*, 2020, **12**, 18409.
24 R. Cancelliere, G. Rea, L. Severini, L. Cerri, G. Leo, E. Paialunga, P. Mantegazza, C. Mazzuca and L. Micheli, *Green Chem.*, 2023, **25**, 6774.
25 E. Palmieri, F. Maita, A. Pellegrino, G. Avola, M. Distefano and L. Maiolo, *IEEE Int. Work. Metrol. Agric. For. MetroAgriFor 2023 – Proc. 2023*, 2023, p. 763.
26 E. Palmieri, L. Maiolo, I. Lucarini, A. D. Fattorini, E. Tamburri, S. Orlanducci, R. Calarco and F. Maita, *Adv. Mater. Technol.*, 2024, **9**, 1.
27 T. Vasuphat, K. Tharnthip, D. Donraporn, J. Kittisak, P. Winita, S. Montira, S. Runglawan, M. Kiattikhun, R. Pornchai, T. Pratchaya, S. Yottha, A. Sittipong, D. Alan B. and W. Patnarin, *Int. J. Biol. Macromol.*, 2023, **244**, 125390.
28 B. Das, P. Chokkalingam, P. Masilamani and S. Shukla, *Int. J. Mol. Sci.*, 2023, **24**, 2757.
29 J. Łojewska, P. Miśkowiec, T. Łojewski and L. M. Proniewicz, *Polym. Degrad. Stab.*, 2005, **88**, 512.
30 X. Su, Z. Yang, K. B. Tan, J. Chen, J. Huang and Q. Li, *Carbohydr. Polym.*, 2020, **241**, 116259.
31 A. Etale, A. J. Onyianta, S. R. Turner and S. J. Eichhorn, *Chem. Rev.*, 2023, **123**(5), 2016–2048.
32 S. Wang, Q. Shen, C. Guo and H. Guo, *Membranes*, 2021, **11**, 915.
33 S. Sousa, A. Costa, A. Silva and R. Simões, *Polymers*, 2019, **11**, 1.
34 R. Cancelliere, A. Di Tinno, A. Cataldo, S. Bellucci, S. Kumbhat and L. Micheli, *Microchem. J.*, 2023, **191**, 108868.
35 R. Cancelliere, T. Cosio, E. Campione, M. Corvino, M. P. D'Amico, L. Micheli, E. Signori and G. Contini, *Front. Chem.*, 2023, **11**, 1.
36 D. Diamond, *Analytical Electrochemistry*, 1996.
37 R. Cancelliere, A. Di Tinno, A. M. Di Lellis, G. Contini, L. Micheli and E. Signori, *Biosens. Bioelectron.*, 2022, **213**, 114467.